Available online at www.sciencedirect.com

ScienceDirect

journal homepage: http://www.elsevier.com/locate/euprot

Proteomic and meta-transcriptomic study on lymph node metastasis in gastric cancer

Hiroshi Ichikawa[a,b], *Tatsuo Kanda*[c], *Shin-ichi Kosugi*[b], *Yasuyuki Kawachi*[d], *Toshifumi Wakai*[b], *Tadashi Kondo*[a,*]

[a] *Division of Pharmacoproteomics, National Cancer Center Research Institute, 5-1-1 Tsukiji, Chuo-ku, Tokyo 104-0045, Japan*

[b] *Division of Digestive and General Surgery, Niigata University Graduate School of Medical and Dental Sciences, 1-757, Asahimachidori, Chuo-ku, Niigata-shi, Niigata 951-8510, Japan*

[c] *Tsubame Rosai Hospital, 633, Sado, Tsubame-shi, Niigata 959-1228, Japan*

[d] *Nagaoka Chuo General Hospital, 2041, Kawasakimachi, Nagaoka-shi, Niigata 940-8653, Japan*

ARTICLE INFO

Article history:
Received 28 November 2013
Received in revised form
21 February 2014
Accepted 10 March 2014
Available online 15 March 2014

Keywords:
Gastric cancer
Lymph node metastasis
Label-free proteomics
Beta-3 integrin
Transcriptome

ABSTRACT

To examine the proteomic background of lymph node metastasis (LNM) in gastric cancer, we performed protein expression profiling of paired non-tumor, primary tumor, and LNM tissues. Using a label-free proteomic approach, we generated protein expression profiles of 3894 unique proteins and identified 109 differentially expressed proteins. Functional pathway analysis of the differentially expressed proteins showed that members of the beta-3 integrin (ITGB3) pathway were significantly enriched. Aberrations of ITGB3 were reported in various malignancies; however, ITGB3 in LNM tissues has not been examined to date. Different level of ITGB3 expression was confirmed in 20 gastric cancer cases by Western blotting. We analyzed the mRNA levels of the differentially expressed proteins by using a public mRNA expression database; 38.8% of the proteins examined, including those involved in oxidation and reduction, showed correlation between protein and mRNA levels. Proteins without such correlation included factors related to cell adhesion. Our study suggests a novel role for the integrin pathway in the development of LNM in gastric cancer and indicated possible benefits of observational transcriptomic analysis for proteomic studies.

1. Introduction

Gastric cancer is the fourth most common cancer and the second leading cause of cancer-related deaths worldwide [1]. Lymph node metastasis (LNM) is an early event of the metastatic process and is most commonly observed in metastatic gastric cancer [2,3]. The LNM status is one of the most important prognostic factors for gastric cancer, and the 5-year survival rate for LNM-positive gastric cancer is 33.2% [4,5]. These observations suggest that the understanding of the molecular mechanisms of LNM can lead to a novel

* *Corresponding author at*: Division of Pharmacoproteomics, National Cancer Center Research Institute, 5-1-1 Tsukiji, Chuo-ku, Tokyo 104-0045, Japan. Tel.: +81 3 3542 2511x3004; fax: +81 3547 5298.
E-mail address: takondo@ncc.go.jp (T. Kondo).

http://dx.doi.org/10.1016/j.euprot.2014.03.001

prognostic indicator or therapeutic approach for the treatment of gastric cancer.

Metastasis of tumor cells consists of multiple selection steps. Subpopulations of cancer cells with high metastatic potential may migrate from the primary site to distant tissues, where cells adaptive to foreign microenvironments clonally proliferate in metastatic sites [6]. To elucidate the molecular mechanisms underlying these multistage events, genome-wide screening has been performed to identify genetic differences between the primary tumors and the LNM tissues in gastric cancer [7,8]. These studies have suggested the existence of complex genetic abnormalities related to gastric cancer metastasis.

The proteome is a functional translation of the genome. The genomic aberrations of cancer cells are transcribed to the transcriptome, translated to the proteome, then determining cancer phenotypes. In this sense, the proteome is a functional translation of the genome, directly regulating tumor behavior. Proteomic studies can generate unique data about the final products of genome information. The proteomic study has been employed to elucidate the mechanisms underlying LNM development in several types of cancers, and various intriguing findings have been reported [9]. Therefore, the investigations by the proteomic approach will be important clues to understand the molecular mechanisms underlying LNM in gastric cancer. These approaches will further the understanding of biological mechanisms in gastric cancer progression and will eventually benefit cancer patients.

In this study, we aimed to elucidate the proteomic background of LNM in gastric cancer. Protein expression profiles consisting of 3894 unique proteins were generated using sodium dodecyl sulfate (SDS)-PAGE-based protein separation followed by LC–MS/MS. Using a label-free quantification method, we identified 109 differentially expressed proteins in the LNM tissues. Functional pathway analysis demonstrated that proteins involved in the beta-3 integrin (ITGB3) pathway were significantly enriched within LNM, and the expression pattern of ITGB3 in gastric cancer progression and metastasis was examined by Western blotting. The application of meta-transcriptomics revealed the possible trends of proteins with concordant and discordant expression between proteins and mRNA.

2. Material and methods

2.1. *Clinical samples*

This study included 20 patients with gastric cancer. Matched and unmatched pairs of tumors, non-tumor and LNM tissues were used; paired tissues from two cases were used for proteomic studies, and all samples were used for Western blotting. The patients underwent surgery at Niigata University Medical and Dental Hospital and the affiliated institutions in Niigata prefecture (Nagaoka Chuo General Hospital, Nanbugo General Hospital, Nagaoka Red Cross Hospital, Nippon Dental University Medical Hospital, Niigata City General Hospital, Tachikawa General Hospital, Shibata Hospital, Saiseikai Niigata Daini Hospital, Sakamachi Hospital, Kashiwazaki General Hospital and Medical Center). All patients underwent surgical resection in 2010 and had no history of cancer treatments involving systemic therapy. At the time of surgery, tissue fragments were grossly resected from the primary tumors, and the matched non-tumor mucosa tissues located at least 5 cm away from the tumor margins were collected. All the tissues were immediately snap-frozen in liquid nitrogen and stored at −80 °C until use. The LNM tissues were cut into two pieces; one was embedded in OCT compound (Sakura Finetechnical, Tokyo, Japan) for histological identification of tumor metastasis, and another was used for proteomic study and Western blotting. By staining frozen sections with hematoxylin–eosin, we confirmed that the lymph node metastatic tissues had at least 50% tumor cells. The tumors were classified on the basis of the histological stage, according to the International Union against Cancer tumor-node-metastasis (TNM) classification, 7th edition [10]. The clinicopathological data for 20 cases are presented in Table 1. This study was approved by the Ethical Review Board of the Niigata University Faculty of Medicine, the affiliated institutions of Niigata University Medical and Dental Hospital, and National Cancer Center. Informed consent was obtained from all the patients at each institution.

2.2. *Protein expression profiling*

Frozen samples were crushed to powder in liquid nitrogen with a Multi-beads shocker (Yasui Kikai, Osaka, Japan) and treated with lysis buffer containing 6 M urea, 2 M thiourea, 3% CHAPS, and 1% Triton X-100. After the mixtures were centrifuged at 15,000 rpm for 30 min, the supernatants were recovered and used in subsequent protein expression studies.

Protein expression profiles were generated by the LC–MS/MS method. Sixty micrograms of each protein sample was separated on a ready-made 12.5% SDS-PAGE gel (ATTO, Tokyo, Japan). Each gel lanes were cut into 48 pieces of equal size by GridCutter (Gel Company, San Francisco, CA) and subjected to in-gel tryptic digestion as described previously [11]. Trypsin digests were subjected to liquid chromatography coupled with analysis with a LTQ-Orbitrap XL mass spectrometer (Thermo Fisher Scientific, San Jose, CA). Acquired MS and MS/MS spectra (Thermo raw files) were analyzed with the Progenesis LC-MS software, version 3.4 (Nonlinear, Dynamics, Newcastle, UK). Profile data of MS scans were transformed to peak lists with respective peak m/z values, intensities, abundances (areas under the peaks), and m/z width. MS/MS spectra were treated similarly.

After selecting one sample as the reference, the retention times of all the other samples used in the experiment were aligned by manually creating three to five landmarks, followed by automatic alignment of all retention times to maximal overlay of the 2D feature maps. Features with only two or three charges were included in further analyses. MS/MS spectra were exported from the Progenesis software as Mascot generic files (mgf) and were used for peptide identification by searching the SWISS-PROT database (*Homo sapiens*, 471,472 sequences in the Sprot_57.5.fasta file) by using the Mascot software (version 2.2; Matrix Science, London, UK). The following search parameters were used: tolerance of two missed trypsin cleavages, variable modifications on the methionine residue (oxidation, +16 Da), maximum precursor ion mass tolerance

Table 1 – Clinical and pathological data of the gastric cancer patients who participated in this study.

Case number[a]	Patient age	Patient sex	Histological differentiation	T status[b]	N status[b]	M status[b]	Number of metastatic nodes	Lymphatic invasion	Vascular invasion	TNM stage[b]
1	76	Male	WD	T4	N3	M1	9	Presence	Presence	IV
2	65	Male	MD	T4	N1	M1	2	Presence	Presence	IV
3	81	Male	WD	T1	N0	M0	0	Absence	Absence	I
4	68	Male	WD	T1	N0	M0	0	Absence	Absence	I
5	70	Male	MD	T2	N0	M0	0	Absence	Absence	I
6	63	Male	MD	T2	N0	M0	0	Absence	Absence	I
7	57	Male	WD	T1	N0	M0	0	Absence	Absence	I
8	72	Male	MD	T3	N0	M0	0	Absence	Absence	II
9	63	Male	MD	T3	N0	M0	0	Absence	Absence	II
10	72	Male	MD	T2	N1	M0	1	Presence	Absence	II
11	81	Male	MD	T3	N1	M0	1	Presence	Absence	II
12	76	Male	WD	T3	N1	M0	1	Presence	Presence	II
13	64	Male	MD	T2	N1	M0	1	Presence	Presence	II
14	56	Male	MD	T3	N3	M0	18	Presence	Presence	III
15	77	Male	MD	T3	N3	M0	12	Presence	Presence	III
16	55	Male	MD	T3	N2	M0	3	Absence	Absence	III
17	76	Male	MD	T3	N3	M0	7	Presence	Presence	III
18	75	Male	MD	T3	N2	M0	3	Absence	Presence	III
19	72	Male	MD	T4	N3	M1	11	Presence	Presence	IV
20	70	Male	WD	T4	N3	M1	12	Presence	Presence	IV

WD, well differentiated; MD, moderately differentiated.

[a] The samples in case 1 and 2 were used to create the protein expression profiles, and those in case 1 to20 were used for Western blotting analysis.

[b] T status, N status, M status and TNM stage were determined according to the International Union against Cancer tumor-node-metastasis (TNM) classification of 7th edition.

of ±10 ppm, and fragment ion mass tolerance of ±0.8 Da. Proteins with a Mascot score of 34 or more were considered as positively identified. Peptide search results were re-imported to the Progenesis software.

For protein quantification, only nonconflicting peptides (i.e., peptides occurring in only one protein) were selected. After summing up the abundances of all the peptides allocated to each protein, the results of 48 fractions were combined in a total analysis set. All the experiments were performed in duplicates, and each number represented an average of two replicates. The processed raw data on protein abundances were normalized by fixing the mean intensity of each sample at one and were presented as a scatter plot; the ratios of mean abundances in two cases between tissue types were calculated using the Expressionist analyst software (GeneData, Basel, Switzerland). We defined the different expression as more than 2.0-fold difference of the mean protein abundance between tissue types. Proteins that showed higher expression in tumor than non-tumor tissues, and also higher expression in LNM than in the tumor tissues, or proteins that showed lower expression in tumors than in the non-tumor tissues, and even lower expression in the LNM tissues were selected as candidate proteins associated with LNM.

2.3. *Pathway analysis*

Pathway analysis of differentially expressed proteins was performed using the Cytoscape software [12] with the Reactome functional interaction (FI) plug-in [13]. The Reactome FI dataset unites interactions from Reactome and those derived from the pathway databases, including KEGG, BioCye, Panther, The Cancer Cell Map (http://cancer.cellmap.org/), and NCI-PID, with pair-wise interactions gleaned from physical protein-protein interactions in human and model organisms, gene coexpression data, protein domain–domain interactions, protein interactions generated from text mining, and GO annotations [13]. To investigate the functions of the network created, pathway enrichment analysis was performed using the Reactome FI plug-in. Pathways with a false discovery rate (FDR) < 0.05 were considered to be significantly enriched.

2.4. *Western blotting*

Protein samples were separated by SDS-PAGE and blotted onto a PVDF membrane. Primary antibodies against ITGB3 (1:1000; BD Bioscience, San Jose, CA) and secondary antibodies against mouse IgG (1:2000, GE Healthcare Biosciences, Uppsala, Sweden) were used, and immunocomplexes were detected using an enhanced chemiluminescence system (ECL Prime Western Blotting Detection Reagents; GE Healthcare Biosciences) and LAS-3000 (Fujifilm, Tokyo, Japan). To normalize the amount of protein loaded in each lane, the same membranes were stained with Ponceau S. The intensity of Western Blot signals and the density of the total lanes stained with Ponceau S were measured using ImageQuant software (GE Healthcare Biosciences), and the relative intensity was calculated by dividing the intensity of Western Blot signals by the optical density of the total lanes.

2.5. *Gene expression analysis*

The microarray and clinical and pathological dataset of 89 gastric cancer cases was obtained from the Gene Expression Omnibus (GEO) database (GSE 4007). This dataset consists of a total of 44,500 probes corresponding to about 30,300 unique genes. Gene expression data of 14 cases that included 14 primary tumor tissues, 14 corresponding LNM tissues, and 5 matched non-tumor mucosae, were selected for the analysis. To compare protein and mRNA expression, we selected probes corresponding to the differentially expressed 109 genes identified in proteomic analysis. We could obtain the expression data of 67 genes. We selected a probe with the highest expression value when multiple ones exist for the identical gene. Additional data processing such as normalization was not performed. Gene expression data were imported to the Expressionist analyst software (GeneData, Basel, Switzerland), and mean expression ratios between different tissue types were calculated. We defined the different expression as more than 1.0 fold difference of the mean expression value between the tissue types.

2.6. *Gene ontology enrichment analysis*

Gene ontology (GO) enrichment analysis was performed using DAVID, version 6.7 [14]. Data related to genes with concordant and discordant mRNA and protein expression were separately uploaded to DAVID, and the background was defined as "*Homo sapiens*". Functional annotation charts were created using "GOTERM_BP_FAT" (collection of broadest GO terms curated from GO annotations dataset). Thresholds were changed to a gene count of two and an EASE score of one (modified Fisher exact *P*-value). The *P*-value for each GO term reflects enrichment in the frequency of that GO term in the uploaded gene list, relative to all the genes in the background list. The GO terms were filtered to include enrichments with Benjamini–Hochberg corrected *P*-values less than 0.20.

2.7. *Statistical analysis*

The Kruskal–Wallis test was performed to compare continuous variables in multiple groups by using the SPSS 11.5 statistical package (SPSS, Chicago, IL), and differences with $P < 0.05$ were considered statistically significant.

3. Results

An overview of the experiment workflow is shown in Fig. 1. First, we generated protein expression profiles of paired non-tumor, tumor, and LNM tissues from cases 1 and 2 (Fig. 1, Table 1). Each protein sample was separated by SDS-PAGE, and the gel lanes were cut to obtain 48 pieces. Trypsin digests were extracted from each gel piece, and subjected to LC–MS/MS. We identified and quantified 109,949 unique peptides corresponding to 3894 nonredundant proteins from six samples in technical duplicates by the Progenesis LC-MS software (Supplementary Tables 1 and 2). To monitor the reproducibility of the whole process (SDS-PAGE separation, in-gel tryptic digestions, LC–MS/MS, and protein quantification), we generated a

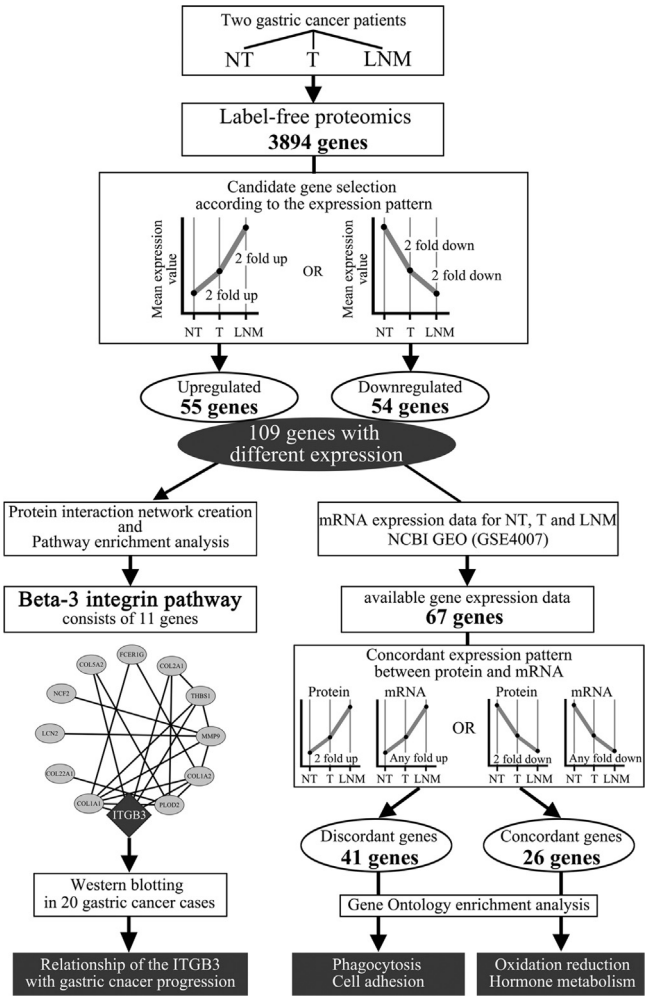

Fig. 1 – Experimental workflow of a label-free proteomics approach with pathway enrichment and mRNA expression meta-analysis. Non-tumor (NT), tumor (T) and lymph node metastasis (LNM) tissues were examined. The label-free quantification method quantified the expression of a total of 3894 proteins; 109 differentially expressed proteins were further analyzed for functional interactions and biological enriched pathways. The beta-3 integrin (ITGB3) pathway was the most enriched pathway in the functional interaction network created. The association between ITGB3 protein expression and gastric cancer progression was confirmed by Western blotting. Among the 109 genes, 67 were grouped according to similarity between the protein and mRNA expression patterns, such as "Concordant genes" or "Discordant genes". Gene ontology analysis showed the enriched functional characteristics in the each gene groups.

scatter plot of technical duplicates from identical samples of the primary tumor tissue from case 2 (Table 1) and calculated the Pearson's correlation coefficient. The scatter plot showed that the normalized abundance of 83.7% and 94.5% of the proteins ranged within 2.0–4.0-fold difference, respectively, and that the correlation coefficient was 0.92 (Supplementary Fig. 1). These results demonstrated high reproducibility of label-free protein expression profiling.

Supplementary Tables 1 and 2 and Fig. 1 can be found, in the online version, at doi:10.1016/j.euprot.2014.03.001.

We compare protein expression profiles between the non-tumor, tumor, and LNM tissues in two cases (Case 1 and 2, Table 1). Among the 3894 proteins, 55 proteins showed significantly (>2-fold ratio of means in two cases) higher expression in tumor than non-tumor tissues and also significantly higher expression in LNM than in the tumor tissues (Fig. 2). In contrast, 54 proteins showed significantly (<2-fold ratio of means in two cases) lower expression in tumors than in the non-tumor tissues, and even significantly lower expression in the LNM tissues (Fig. 3). We selected the 109 differentially expressed proteins as candidate proteins associated with LNM. Details of these proteins are presented in Supplementary Table 3.

Supplementary Table 3 can be found, in the online version, at doi:10.1016/j.euprot.2014.03.001.

We studied the functional interactions of these 109 proteins by using Cytoscape with the Reactome FI plug-in. We found that 11 (10.1%) of the 109 proteins were functionally linked to each other and that the ITGB3 cell surface interactions pathway was the most significantly enriched in the identified network of the 11 proteins (FDR < 1.00E-4, Fig. 4A and Table 2). ITGB3 was identified and examined in our proteomic analysis. ITGB3 protein expression in the LNM tissues was lower than that of the tumor tissues (ratio of means = 3.96), and that of the tumor tissues was higher than that of the non-tumor tissues (ratio of means = 1.76) (Fig. 4B). We validated the relationship between ITGB3 expression and gastric cancer progression in 20 cases by Western blotting. ITGB3 expression was found to significantly increase with cancer stage progression but decrease in LNM tissues (Fig. 4C). These observations confirmed the results of the label-free protein expression profiling.

We analyzed the mRNA levels for the 109 differentially expressed proteins by using a public mRNA expression database. We selected the GSE4007 dataset in the NCBI Gene Expression Omnibus (GEO) because it was the only dataset that included mRNA expression data obtained from paired non-tumor tissues, primary tumor tissues, and LNM tissues, along with sufficient clinical information. From the 109 genes, the mRNA expression data for 67 genes were included in the GSE4007 dataset. Clinical and pathological information and data on mRNA expression have been presented in Supplementary Tables 4 and 5, respectively.

Supplementary Tables 4 and 5 can be found, in the online version, at doi:10.1016/j.euprot.2014.03.001.

To characterize the genes according to the correlation between mRNA and protein expression, we divided the 67 genes into two groups: 26 genes (38.8%) that showed the same protein and mRNA expression patterns were grouped into "Concordant genes" (Table 3), whereas 41 genes that showed different patterns were grouped into "Discordant genes". We analyzed the enriched GO terms in each group by using DAVID, version 6.7. GO terms related to oxidation, reduction, or hormone metabolism were enriched in the group of "Concordant genes", while those involved in phagocytosis or cell adhesion

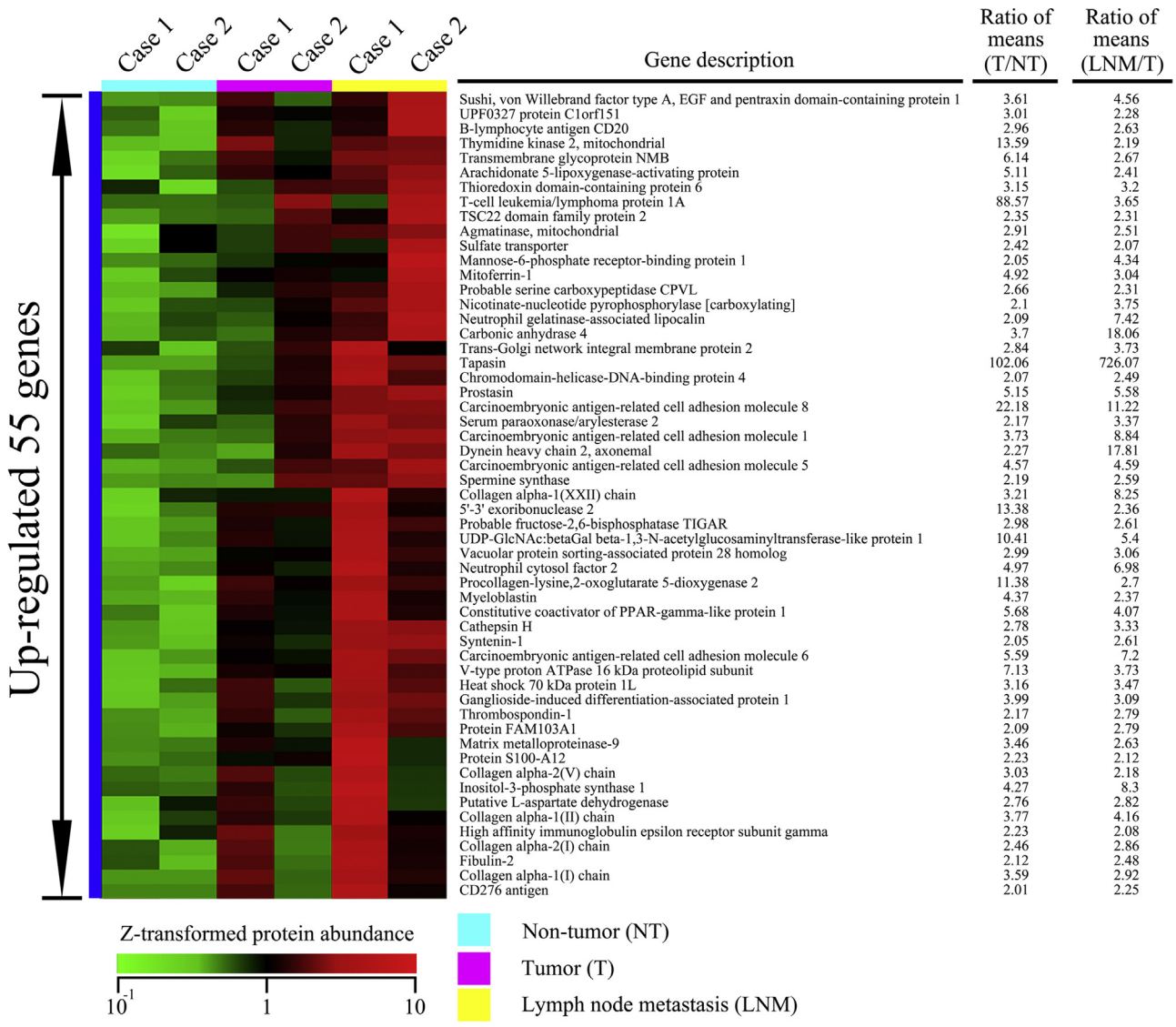

Gene description	Ratio of means (T/NT)	Ratio of means (LNM/T)
Sushi, von Willebrand factor type A, EGF and pentraxin domain-containing protein 1	3.61	4.56
UPF0327 protein C1orf151	3.01	2.28
B-lymphocyte antigen CD20	2.96	2.63
Thymidine kinase 2, mitochondrial	13.59	2.19
Transmembrane glycoprotein NMB	6.14	2.67
Arachidonate 5-lipoxygenase-activating protein	5.11	2.41
Thioredoxin domain-containing protein 6	3.15	3.2
T-cell leukemia/lymphoma protein 1A	88.57	3.65
TSC22 domain family protein 2	2.35	2.31
Agmatinase, mitochondrial	2.91	2.51
Sulfate transporter	2.42	2.07
Mannose-6-phosphate receptor-binding protein 1	2.05	4.34
Mitoferrin-1	4.92	3.04
Probable serine carboxypeptidase CPVL	2.66	2.31
Nicotinate-nucleotide pyrophosphorylase [carboxylating]	2.1	3.75
Neutrophil gelatinase-associated lipocalin	2.09	7.42
Carbonic anhydrase 4	3.7	18.06
Trans-Golgi network integral membrane protein 2	2.84	3.73
Tapasin	102.06	726.07
Chromodomain-helicase-DNA-binding protein 4	2.07	2.49
Prostasin	5.15	5.58
Carcinoembryonic antigen-related cell adhesion molecule 8	22.18	11.22
Serum paraoxonase/arylesterase 2	2.17	3.37
Carcinoembryonic antigen-related cell adhesion molecule 1	3.73	8.84
Dynein heavy chain 2, axonemal	2.27	17.81
Carcinoembryonic antigen-related cell adhesion molecule 5	4.57	4.59
Spermine synthase	2.19	2.59
Collagen alpha-1(XXII) chain	3.21	8.25
5'-3' exoribonuclease 2	13.38	2.36
Probable fructose-2,6-bisphosphatase TIGAR	2.98	2.61
UDP-GlcNAc:betaGal beta-1,3-N-acetylglucosaminyltransferase-like protein 1	10.41	5.4
Vacuolar protein sorting-associated protein 28 homolog	2.99	3.06
Neutrophil cytosol factor 2	4.97	6.98
Procollagen-lysine,2-oxoglutarate 5-dioxygenase 2	11.38	2.7
Myeloblastin	4.37	2.37
Constitutive coactivator of PPAR-gamma-like protein 1	5.68	4.07
Cathepsin H	2.78	3.33
Syntenin-1	2.05	2.61
Carcinoembryonic antigen-related cell adhesion molecule 6	5.59	7.2
V-type proton ATPase 16 kDa proteolipid subunit	7.13	3.73
Heat shock 70 kDa protein 1L	3.16	3.47
Ganglioside-induced differentiation-associated protein 1	3.99	3.09
Thrombospondin-1	2.17	2.79
Protein FAM103A1	2.09	2.79
Matrix metalloproteinase-9	3.46	2.63
Protein S100-A12	2.23	2.12
Collagen alpha-2(V) chain	3.03	2.18
Inositol-3-phosphate synthase 1	4.27	8.3
Putative L-aspartate dehydrogenase	2.76	2.82
Collagen alpha-1(II) chain	3.77	4.16
High affinity immunoglobulin epsilon receptor subunit gamma	2.23	2.08
Collagen alpha-2(I) chain	2.46	2.86
Fibulin-2	2.12	2.48
Collagen alpha-1(I) chain	3.59	2.92
CD276 antigen	2.01	2.25

Fig. 2 – Fifty-five significantly upregulated proteins identified by a label-free quantification method. The protein abundance in each case was z-transformed across all six samples and has been presented in a heatmap format. Tissue types are marked as non-tumor (NT), tumor (T), and lymph node metastasis (LNM). Case numbers correspond to those in Table 1 and Fig. 4. Refer to Supplementary Table 3 for the gene description and values of the ratio of means.

were over-represented in the "Discordant genes" group (Fig. 5 and Supplementary Table 6).

Supplementary Table 6 can be found, in the online version, at doi:10.1016/j.euprot.2014.03.001.

4. Discussion

LNM is one of the most important prognostic factors in gastric cancer, and investigation of the molecular background of LNM formation may lead to novel therapeutic modalities [4]. Metastasis has been assumed to occur through clonal genomic and epigenetic evolution [5]. Molecular mechanisms related to tumor metastasis are upregulated in metastatic tumor cells compared to primary tumors, and exploring differences in the molecular background of primary tumors and LNM tissues may be the most direct and credible way to elucidate the molecular mechanisms underlying the metastasis process.

We employed SDS-PAGE-based size fractionation before mass spectrometry analysis. Pre-fractionation of proteins by SDS-PAGE has significant advantages over other separation techniques in that it detects a greater number of proteins and is widely used to characterize protein complexes in cancer proteomic studies [15–17]. Gel-based size fractionation for the identification of proteins is superior to separation by liquid chromatography as a pre-fractionation method [18]. Jafari et al. compared gel-based protein-separation techniques, including SDS-PAGE, isoelectric focusing with immobilized pH gradient gel strips (IEF-IPG), and two-dimensional PAGE (2D-PAGE), on the basis of their ability to serve as a

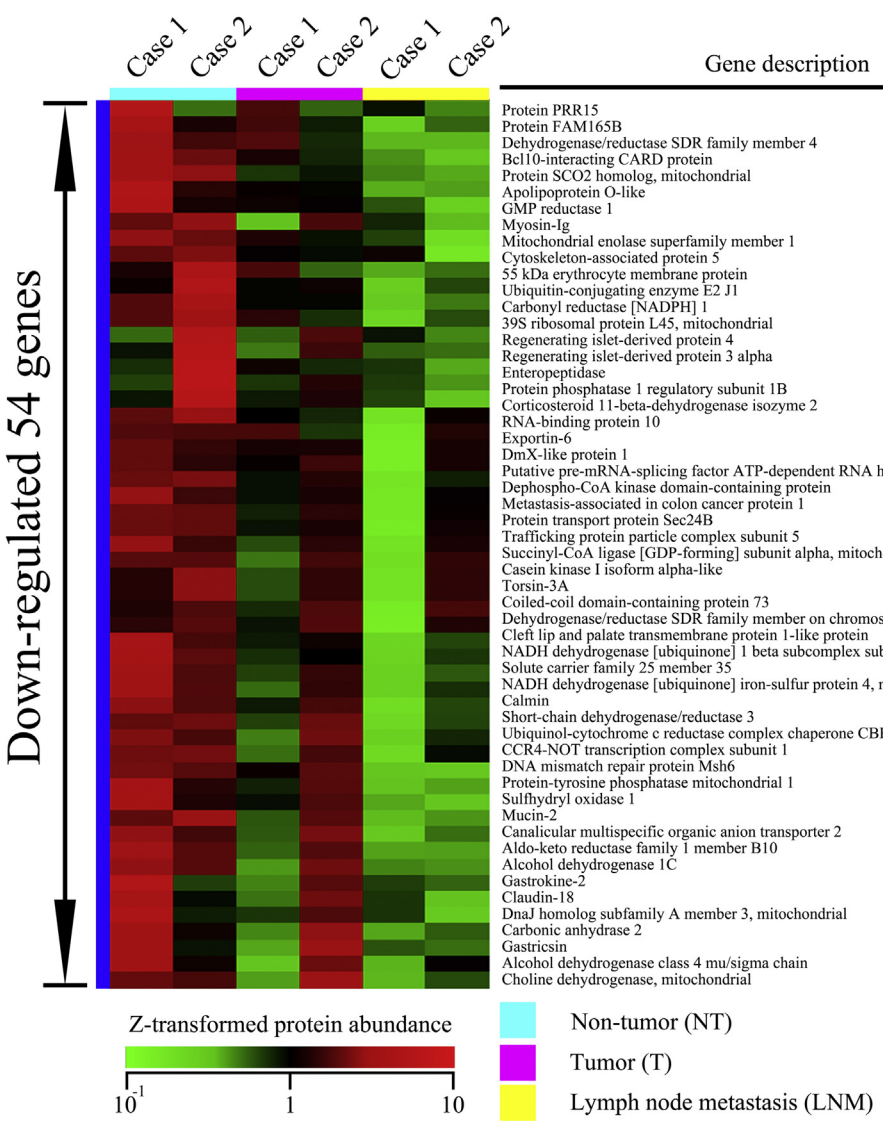

Gene description	Ratio of means (T/NT)	Ratio of means (LNM/T)
Protein PRR15	4.33E-01	4.87E-01
Protein FAM165B	4.56E-01	2.54E-01
Dehydrogenase/reductase SDR family member 4	4.87E-01	2.76E-01
Bcl10-interacting CARD protein	4.46E-01	4.67E-01
Protein SCO2 homolog, mitochondrial	4.10E-02	2.43E-01
Apolipoprotein O-like	4.63E-01	4.57E-01
GMP reductase 1	4.07E-01	3.27E-01
Myosin-Ig	1.04E-02	2.16E-01
Mitochondrial enolase superfamily member 1	4.37E-01	3.56E-01
Cytoskeleton-associated protein 5	3.19E-02	4.01E-02
55 kDa erythrocyte membrane protein	3.70E-01	4.06E-01
Ubiquitin-conjugating enzyme E2 J1	3.81E-01	3.33E-01
Carbonyl reductase [NADPH] 1	4.60E-01	4.98E-01
39S ribosomal protein L45, mitochondrial	4.44E-01	4.25E-01
Regenerating islet-derived protein 4	4.92E-01	4.95E-01
Regenerating islet-derived protein 3 alpha	1.96E-01	3.85E-01
Enteropeptidase	3.72E-01	4.94E-01
Protein phosphatase 1 regulatory subunit 1B	3.50E-01	4.12E-01
Corticosteroid 11-beta-dehydrogenase isozyme 2	3.70E-01	3.27E-01
RNA-binding protein 10	2.81E-01	4.70E-01
Exportin-6	3.68E-01	1.97E-01
DmX-like protein 1	2.71E-01	2.47E-02
Putative pre-mRNA-splicing factor ATP-dependent RNA helicase DHX32	3.06E-01	9.80E-03
Dephospho-CoA kinase domain-containing protein	3.78E-01	2.46E-01
Metastasis-associated in colon cancer protein 1	3.32E-01	2.47E-01
Protein transport protein Sec24B	3.57E-01	2.72E-01
Trafficking protein particle complex subunit 5	3.42E-01	2.78E-01
Succinyl-CoA ligase [GDP-forming] subunit alpha, mitochondrial	3.92E-01	4.97E-01
Casein kinase I isoform alpha-like	2.03E-02	8.49E-02
Torsin-3A	4.11E-01	4.95E-01
Coiled-coil domain-containing protein 73	4.11E-01	4.95E-01
Dehydrogenase/reductase SDR family member on chromosome X	3.16E-01	4.36E-02
Cleft lip and palate transmembrane protein 1-like protein	4.70E-01	5.37E-02
NADH dehydrogenase [ubiquinone] 1 beta subcomplex subunit 3	4.26E-01	4.61E-01
Solute carrier family 25 member 35	2.41E-01	4.28E-01
NADH dehydrogenase [ubiquinone] iron-sulfur protein 4, mitochondrial	4.18E-01	4.21E-01
Calmin	2.91E-01	4.71E-01
Short-chain dehydrogenase/reductase 3	3.98E-01	1.68E-01
Ubiquinol-cytochrome c reductase complex chaperone CBP3 homolog	3.88E-01	1.72E-01
CCR4-NOT transcription complex subunit 1	4.46E-01	4.10E-01
DNA mismatch repair protein Msh6	2.58E-01	3.55E-01
Protein-tyrosine phosphatase mitochondrial 1	1.44E-01	4.00E-04
Sulfhydryl oxidase 1	4.61E-01	2.01E-01
Mucin-2	4.04E-01	3.47E-01
Canalicular multispecific organic anion transporter 2	4.72E-01	2.75E-01
Aldo-keto reductase family 1 member B10	3.08E-01	3.01E-01
Alcohol dehydrogenase 1C	4.24E-01	4.79E-01
Gastrokine-2	3.76E-01	4.97E-01
Claudin-18	3.91E-01	2.98E-01
DnaJ homolog subfamily A member 3, mitochondrial	4.04E-01	2.20E-01
Carbonic anhydrase 2	4.61E-01	2.99E-01
Gastricsin	4.34E-01	3.00E-01
Alcohol dehydrogenase class 4 mu/sigma chain	1.94E-02	2.00E-01
Choline dehydrogenase, mitochondrial	4.64E-01	3.20E-01

Fig. 3 – Fifty-four significantly downregulated proteins identified by a label-free quantification method. The protein abundance of each gene was z-transformed across all 6 samples and has been presented in a heatmap format. The tissue types are marked as shown in Fig. 2. Case numbers correspond to those in Table 1 and Fig. 4. Refer to Supplementary Table 3 for the gene description and values of the ratio of means.

fractionation technique for MS analysis of a complex protein sample [19]. They reported that SDS-PAGE yielded the highest number of identifiable proteins.

In addition, we quantified the identified proteins by a label-free method with the Progenesis LC-MS software. Label-free quantification is widely used because it is a simple technique that allows simultaneous identification and quantification of proteins. Alternatively, isotopic labeling methods such as ICAT [20], iTRAQ [21], and SILAC [22] are also used for MS-based protein quantification; these isotopic labeling methods allow for the comparison of multiple samples in a single LC–MS/MS run, thereby providing increased accuracy, precision, and reproducibility [23]. However, such experiments are complicated because of the additional labeling reactions, and SILAC is available only in tissue culture systems. A label-free method based on Progenesis LC-MS can quantify and identify thousands of proteins from complex samples with a simple technique and high reproducibility. Progenesis LC-MS aligns the ion chromatograms to compensate for variations in retention times among multiple samples before quantification based on ion intensities. It has been reported that analysis of retention time alignment shows similar quantification precision and reproducibility but higher identification capacity than isotope labeling methods such as SILAC [24]. In this study, we identified and quantified 3894 non-redundant proteins from complex clinical samples with high reproducibility (Supplementary Fig. 1) and then employed a label-free quantification method for the proteomic studies.

The development of tumor invasion and metastasis is a very complicated and continuous process with multi steps.

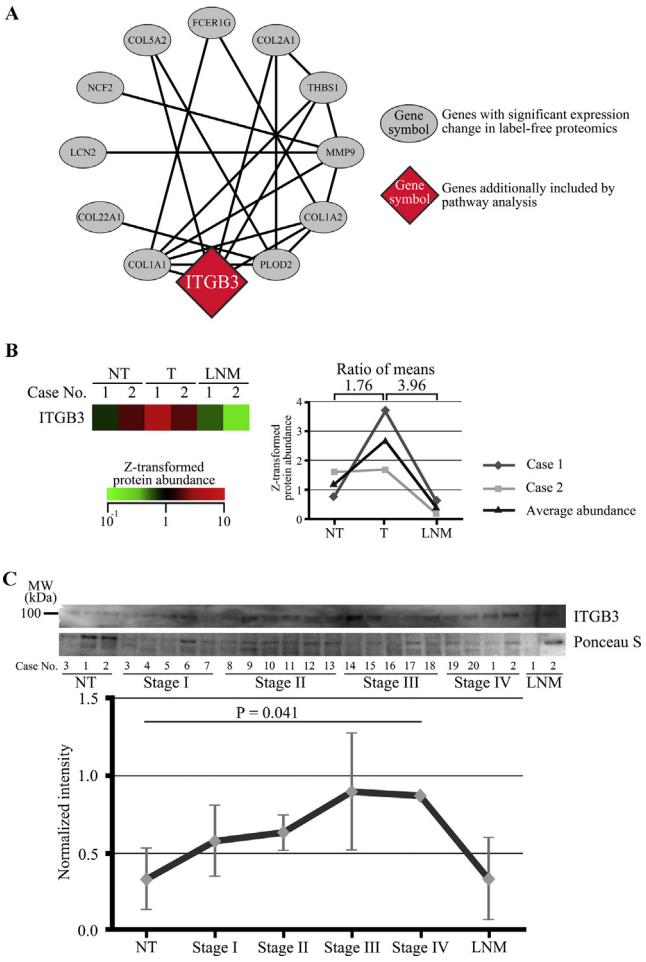

Fig. 4 – Beta-3 integrin (ITGB3) pathway and association of the ITGB3 protein expression with progression of gastric cancer. Case numbers corresponded to those in Table 1. Functional interaction network analysis by Cytoscape with the Reactome FI plug-in is demonstrated (A). The ITGB3 protein expression level quantified by a label-free method (B). ITGB3 protein expression level was z-transformed across all six samples examined and was represented as a heat-map format and line chart. ITGB3 protein expression in 20 gastric cancer cases, evaluated by Western blotting (C).

Investigation of the molecular background of tumor metastasis through "omics" studies revealed that multiple genes aberrations were contributed to the tumor metastasis [7,8]. Therefore, we tried to examine the overall features of the expressed proteins, and identified 109 aberrantly expressed proteins. Next, we identified the ITGB3 pathway as the most enriched protein interaction network thorough the pathway enrichment analysis in the 109 proteins (Fig. 4A). In addition, we monitored the ITGB3 protein expression using the created protein expression profile. Integrins are heterodimeric cell surface glycoproteins with alpha and beta subunits. ITGB3 expression is mainly associated with the migration and invasion of tumor cells [25], and overexpression of ITGB3 is related to the metastatic potential of melanoma [26], breast cancer [27], colorectal cancer [28], and bone metastasis in breast cancer [29]. However, in ovarian cancer, ITGB3 reduces the metastatic potential of tumor cells [30–32]. In hepatocellular carcinoma cells, ITGB3 has been shown to have a proapoptotic function, and downregulation of ITGB3 is related to aggressive tumor growth [33]. Therefore, the association of ITGB3 expression with tumor metastasis and progression depends on the cancer type. In the current study, ITGB3 expression was increased as cancer stage advanced, thereby linking it to gastric cancer progression. These observations are supported by previous findings [34]. However, downregulation of ITGB3 in the LNM tissues has not been reported until our study. Neoplastic invading cells must overcome the integrin-mediated death (IMD) induced by the interaction of ITGB3 with the extracellular matrix of host tissues to establish metastases [25]. When a tumor cell migrates through a microenvironment where the extracellular matrix (ECM) does not contain a suitable ligand for ITGB3, the integrin cytoplasmic tail recruits caspase-8 to the cell membrane, and apoptosis is induced. Stupack et al. [35] showed that ITGB3-expressing melanoma cells undergo apoptosis in collagen gels that lack ITGB3 ligands. ITGB3 specifically binds a wide range of ECM molecules, including fibronectin, fibrinogen, von Willebrand factor, and vitronectin [36]. The present proteomic analysis demonstrated that several collagen-related genes were upregulated in LNM tissues, while fibronectin, fibrinogen, and vitronectin were not identified as upregulated proteins in LNM tissues (Fig. 2 and Supplementary Table 3). Therefore, ITGB3 downregulation in gastric cancer cells that showed LNM might reflect a survival mechanism related to the prevention of IMD in metastatic tissues.

The problems of the proteomic biomarker studies are lack of the validation studies in the independent clinical samples from the multi-institutions. Selection of biomarker candidates from the differentially expressed proteins and acquisition of the independent clinical samples are critical steps in multi-institutional biomarker validation studies. Transcriptome data are deposited in public databases with clinicopathological data of the samples, and are freely available for independent validation studies; as clinical materials are generally not very accessible, such infrastructure is highly desirable for proteomic biomarker studies. However, presently, there is no analogous proteomic database. For proteins whose levels demonstrate concordance with mRNA expression, a transcriptome database should be a useful tool for biomarker selection and validation. Several studies have compared mRNA and protein levels in tissue culture cells. Chen et al. [37] compared mRNA and protein expression between two gastric cancer cell lines and estimated an overall correlation coefficient of 0.29. Previous studies comparing mRNA and protein expression in human and mouse cell lines concluded that the mRNA levels explain approximately 40% of the variability in protein levels [38]. Although these studies suggested possible benefits of using transcriptome databases for validation studies, the correlation between protein and mRNA expression in surgically resected tissues remain unclear. We analyzed the mRNA levels for the 109 differentially expressed proteins by using a public mRNA expression database. Of these 109 proteins, 67 were listed in the gastric cancer dataset of the GEO database. We found that 26 of 67 genes (38.8%) showed a concordant expression pattern for protein and mRNA. These concordant genes were enriched in GO terms related to

Table 2 – Pathway enrichment analysis for the identified protein network consisting of 11 proteins.

Pathway[a]	Source[b]	FDR[c]	Number of proteins[d]	Included proteins[e]
Beta3 integrin cell surface interactions	NCI-PID	1.00E−04	3	COL1A2, COL1A1, THBS1
Amoebiasis	KEGG	1.11E−04	4	COL1A2, COL2A1, COL1A1, COL5A2
Integrin cell surface interactions	Reactome	1.25E−04	4	COL1A2, COL2A1, COL1A1, THBS1
Protein digestion and absorption	KEGG	1.43E−04	4	COL1A2, COL2A1, COL1A1, COL5A2
Signaling by PDGF	Reactome	1.67E−04	5	COL1A2, COL2A1, COL1A1, THBS1, COL5A2
Integrin signaling pathway	Panther	1.82E−04	4	COL1A2, COL2A1, COL1A1, COL5A2
Focal adhesion	KEGG	2.00E−04	5	COL1A2, COL2A1, COL1A1, THBS1, COL5A2
Platelet adhesion to exposed collagen	Reactome	2.50E−04	3	COL1A2, FCER1G, COL1A1
ECM-receptor interaction	KEGG	3.33E−04	5	COL1A2, COL2A1, COL1A1, THBS1, COL5A2
Beta1 integrin cell surface interactions	NCI-PID	5.00E−04	5	COL1A2, COL2A1, COL1A1, THBS1, COL5A2
Extracellular matrix organization	Reactome	1.00E−03	7	PLOD2, MMP9, COL22A1, COL1A2, COL2A1, COL1A1, COL5A2
Cell surface interactions at the vascular wall	Reactome	1.31E−03	3	COL1A2, FCER1G, COL1A1
Axon guidance	Reactome	1.42E−03	4	COL1A2, COL2A1, COL1A1, COL5A2
Platelet activation, signaling and aggregation	Reactome	1.93E−03	4	COL1A2, FCER1G, COL1A1, THBS1
VEGFR3 signaling in lymphatic endothelium	NCI-PID	4.00E−03	2	COL1A2, COL1A1
Syndecan-4-mediated signaling events	NCI-PID	6.06E−03	2	MMP9, THBS1
Validated transcriptional targets of AP1 family members Fra1 and Fra2	NCI-PID	7.76E−03	2	MMP9, COL1A2
Bladder cancer	KEGG	9.39E−03	2	MMP9, THBS1

[a] Pathway enrichment analysis was performed using Cytoscape with Reactome FI plug-in [http://wiki.reactome.org/index.php/Reactome_FI_Cytoscape_Plugin].
[b] Reactome FI data set unites interactions from Reactome and those derived from other pathway databases, including KEGG, NCI-PID, BioCyc, Panther and The Cancer Cell Map.
[c] FDR was calculated by Reactome FI plug-in, and the significant threshold was set at less than 0.05.
[d] The numbers of proteins which were examined in this study involved in the pathway.
[e] Gene names which were identified to be significantly up- or down-regulated by proteomic experiment were shown.

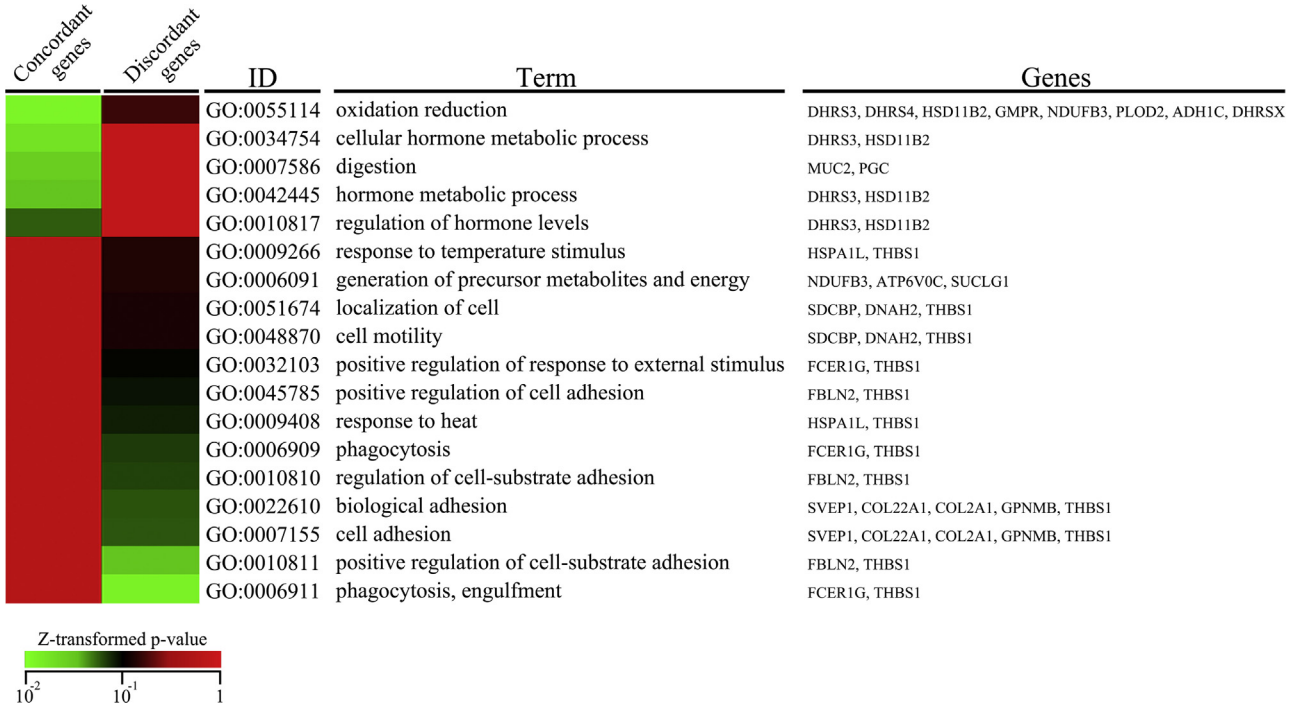

Fig. 5 – Functional characteristics of genes with concordant and discordant protein and mRNA expression. Genes were grouped according to their protein and mRNA expression patterns and analyzed for enriched gene ontology terms by DAVID, version 6.7 (http://david.abcc.ncifcrf.gov). GO terms with enrichment of $P < 0.20$ were listed, and P-values were z-transformed and have been presented in a heatmap format.

Table 3 – List of 26 genes with correlation between protein and mRNA expression.

Gene symbol[a]	Gene ID[b]	Gene description	Protein			mRNA			
			Accession number[c]	Ratio (T/NT)[d]	Ratio (LNM/T)[e]	Probe ID[f]	Accession number[g]	Ratio (T/NT)[d]	Ratio (LNM/T)[e]
Up-regulated genes at both protein and mRNA level									
MMP9	4318	Matrix metalloproteinase-9	P14780	3.46	2.63	10805	T64837	2.56	1.03
AGMAT	79814	Agmatinase, mitochondrial	Q9BSE5	2.91	2.51	15950	AA934764	1.11	1.24
CTSH	1512	Cathepsin H	P09668	2.78	3.33	953	AA487231	1.04	1.05
TGOLN2	10618	Trans-Golgi network integral membrane protein 2	O43493	2.84	3.73	15417	T81338	1.21	1.05
SLC26A2	1836	Sulfate transporter	P50443	2.42	2.07	10913	W15263	1.13	1.02
XRN2	22803	5′–3′ exoribonuclease 2	Q9H0D6	13.38	2.36	8162	AA028164	1.41	1.13
FAM103A1	83640	Protein FAM103A1	Q9BTL3	2.09	2.79	12871	AA432100	1.14	1.01
TAPBP	6892	Tapasin	O15533	102.06	726.07	18291	AA704775	2.20	1.09
TCL1A	8115	T-cell leukemia/lymphoma protein 1A	P56279	88.57	3.65	12786	R97095	1.07	2.62
GDAP1	54332	Ganglioside-induced differentiation-associated protein 1	Q8TB36	3.99	3.09	17310	H15302	1.45	1.06
NCF2	4688	Neutrophil cytosol factor 2	P19878	4.97	6.98	6201	AA872098	3.26	1.42
CHD4	1108	Chromodomain-helicase-DNA-binding protein 4	Q14839	2.07	2.49	5588	N34372	1.16	1.20
Down-regulated genes at both protein and mRNA level									
CA2	760	Carbonic anhydrase 2	P00918	4.61E−01	2.99E−01	15331	H23187	1.21E−01	9.92E−01
GKN2	200504	Gastrokine-2	Q86XP6	3.76E−01	4.97E−01	8090	AI732254	1.45E−02	3.96E−01
MUC2	4583	Mucin-2	Q02817	4.04E−01	3.47E−01	25161	AA534503	4.62E−01	5.30E−01
CLDN18	51208	Claudin-18	P56856	3.91E−01	2.98E−01	11694	AI820565	3.45E−01	6.81E−01
DHRS4	10901	Dehydrogenase/reductase SDR family member 4	Q9BTZ2	4.87E−01	2.76E−01	18212	AA429946	6.46E−01	9.40E−01
DHRS3	9249	Short-chain dehydrogenase/reductase 3	O75911	3.98E−01	1.68E−01	1133	AA171606	7.77E−01	8.00E−01
HSD11B2	3291	Corticosteroid 11-beta-dehydrogenase isozyme 2	P80365	3.70E−01	3.27E−01	174	W95082	6.95E−01	8.90E−01
PGC	5225	Gastricsin	P20142	4.34E−01	3.00E−01	19526	AI674972	3.04E−02	3.25E−01
REG4	83998	Regenerating islet-derived protein 4	Q9BYZ8	4.92E−01	4.95E−01	3562	AA535703	6.40E−01	7.55E−01
PRR15	222171	Protein PRR15	Q8IV56	4.33E−01	4.87E−01	17960	AA515032	8.49E−01	6.52E−01
GMPR	2766	GMP reductase 1	P36959	4.07E−01	3.27E−01	19	AA406242	5.21E−01	9.33E−01
CLMN	79789	Calmin	Q96JQ2	2.91E−01	4.71E−01	23849	AA775028	7.31E−01	8.14E−01
ABCC3	8714	Canalicular multispecific organic anion transporter 2	O15438	4.72E−01	2.75E−01	15480	AA429895	7.51E−01	6.54E−01

[a] Gene symbols were derived from UniGene.
[b] Gene IDs were derived from Entrez Gene database.
[c] Accession numbers of proteins were derived from SWISS-PROT and NCBI nonredundant databases.
[d] Ratios were calculated by dividing the mean expression value of primary tumor samples (T) by that of non-tumor samples (NT).
[e] Ratios were calculated by dividing the mean expression value of lymph node metastasis samples (LNM) by that of primary tumor samples (T).
[f] Probe IDs were derived from NCBI GEO platform (GPL1283).
[g] Accession numbers of genes were derived from GenBank database.

oxidation reduction, or hormone metabolism, while the genes with discordant expression pattern were enriched in GO terms related to phagocytosis and cell adhesion. These results are consistent with the findings of Schwänhausser et al. [38], who reported that genes related to oxidation reduction, and metabolism were enriched in the group with stable and concordant mRNA and protein expression. They also found that the GO terms of cell adhesion were enriched in the group of genes that was characterized by stable mRNA but unstable protein and was expected to have discordant expression [38]. Unfortunately, the reliability of our analysis did not reach their one because the number of samples in our proteomic study was limited and mRNA expression data was obtained from different patient cohorts. Further investigation of additional samples will be required to generalize our observations. The use of public transcriptome databases will solve the problems of proteomic biomarker studies, and therefore, these investigations should be continued.

In our study, highly comprehensive and reproducible proteomic analysis performed using a label-free quantification method showed downregulation of ITGB3 gene expression in the LNM tissues. Downregulation of ITGB3 represents a prosurvival response for overcoming apoptotic IMD at the metastatic site. Further studies on the prognostic and biological significance of ITGB3 may lead to novel risk-stratification approaches for gastric cancer.

Acknowledgements

We would greatly appreciate Dr. M Sasagawa (Nanbugo General Hospital), Dr. N Shimakage (Nagaoka Red Cross Hospital), Dr. T Suda (Nippon Dental University Medical Hospital), Dr. N Katayanagi (Niigata City General Hospital), Dr. T Tada (Tachikawa General Hospital), Dr. S Shimoda (Shibata Hospital), Dr. N Musha (Saiseikai Niigata Daini Hospital), Dr. H Tomita (Sakamachi Hospital) and K Ueki (Kashiwazaki General Hospital and Medical Center) to collect the clinical samples and the clinicopathological data. This work was supported by the National Cancer Center Research Core Facility and the National Cancer Center Research and Development Fund (23-A-8 and 23-A-10). Hiroshi Ichikawa was awardee of Research Resident Fellowship from the Foundation for Promotion of Cancer Research (Japan) for the 3rd Term Comprehensive 10-Year Strategy for Cancer Control.

REFERENCES

[1] Ferlay J, Shin HR, Bray F, Forman D, Mathers C, Parkin DM. Estimates of worldwide burden of cancer in 2008: GLOBOCAN 2008. Int J Cancer 2010;127:2893–917.
[2] Isobe Y, Nashimoto A, Akazawa K, Oda I, Hayashi K, Miyashiro I, et al. Gastric cancer treatment in Japan: 2008 annual report of the JGCA nationwide registry. Gastric Cancer 2011;14:301–16.
[3] Wang W, Li YF, Sun XW, Chen YB, Li W, Xu DZ, et al. Prognosis of 980 patients with gastric cancer after surgical resection. Chin J Cancer 2010;29:923–30.
[4] Park SR, Kim MJ, Ryu KW, Lee JH, Lee JS, Nam BH, et al. Prognostic value of preoperative clinical staging assessed by computed tomography in resectable gastric cancer patients: a viewpoint in the era of preoperative treatment. Ann Surg 2010;251:428–35.
[5] Deng J, Liang H, Sun D, Zhang R, Zhan H, Wang X. Prognosis of gastric cancer patients with node-negative metastasis following curative resection: outcomes of the survival and recurrence. Can J Gastroenterol 2008;22:835–9.
[6] Chaffer CL, Weinberg RA. A perspective on cancer cell metastasis. Science 2011;331:1559–64.
[7] Xie HL, Li ZY, Gan RL, Li XJ, Zhang QL, Hui M, et al. Differential gene and protein expression in primary gastric carcinomas and their lymph node metastases as revealed by combined cDNA microarray and tissue microarray analysis. J Dig Dis 2010;11:167–75.
[8] Liu X-P, Li D-Y, Liu X-L, Xu J-D, Furuya T, Kawauchi S, et al. Comparison of chromosomal aberrations between primary tumors and their synchronous lymph-node metastases in intestinal-type gastric carcinoma. Pathol Res Pract 2009;205:105–11.
[9] Silvestri A, Calvert V, Belluco C, Lipsky M, De Maria R, Deng J, et al. Protein pathway activation mapping of colorectal metastatic progression reveals metastasis-specific network alterations. Clin Exp Metastasis 2013;30:309–16.
[10] Rusch VW, Rice TW, Crowley J, Blackstone EH, Rami-Porta R, Goldstraw P. The seventh edition of the American Joint Committee on Cancer/International Union Against Cancer Staging Manuals: the new era of data-driven revisions. J Thorac Cardiovasc Surg 2010;139:819–21.
[11] Kondo T, Hirohashi S. Application of highly sensitive fluorescent dyes (CyDye DIGE Fluor saturation dyes) to laser microdissection and two-dimensional difference gel electrophoresis (2D-DIGE) for cancer proteomics. Nat Protoc 2007;1:2940–56.
[12] Shannon P, Markiel A, Ozier O, Baliga NS, Wang JT, Ramage D, et al. Cytoscape: a software environment for integrated models of biomolecular interaction networks. Genome Res 2003;13:2498–504.
[13] Croft D, O'Kelly G, Wu G, Haw R, Gillespie M, Matthews L, et al. Reactome: a database of reactions, pathways and biological processes. Nucleic Acids Res 2011;39:D691–7.
[14] Huang da W, Sherman BT, Lempicki RA. Systematic and integrative analysis of large gene lists using DAVID bioinformatics resources. Nat Protoc 2009;4:44–57.
[15] Xie LQ, Zhao C, Cai SJ, Xu Y, Huang LY, Bian JS, et al. Novel proteomic strategy reveal combined alpha1 antitrypsin and cathepsin D as biomarkers for colorectal cancer early screening. J Proteome Res 2010;9:4701–9.
[16] Thakur D, Rejtar T, Wang D, Bones J, Cha S, Clodfelder-Miller B, et al. Microproteomic analysis of 10,000 laser captured microdissected breast tumor cells using short-range sodium dodecyl sulfate-polyacrylamide gel electrophoresis and porous layer open tubular liquid chromatography tandem mass spectrometry. J Chromatogr A 2011;1218:8168–74.
[17] Zhang Y, Xu B, Liu Y, Yao H, Lu N, Li B, et al. The ovarian cancer-derived secretory/releasing proteome: a repertoire of tumor markers. Proteomics 2012;12:1883–91.
[18] Pernemalm M, Orre LM, Lengqvist J, Wikstrom P, Lewensohn R, Lehtio J. Evaluation of three principally different intact protein prefractionation methods for plasma biomarker discovery. J Proteome Res 2008;7:2712–22.
[19] Jafari M, Primo V, Smejkal GB, Moskovets EV, Kuo WP, Ivanov AR. Comparison of in-gel protein separation techniques commonly used for fractionation in mass spectrometry-based proteomic profiling. Electrophoresis 2012;33:2516–26.
[20] Gygi SP, Rist B, Gerber SA, Turecek F, Gelb MH, Aebersold R. Quantitative analysis of complex protein mixtures using isotope-coded affinity tags. Nat Biotechnol 1999;17:994–9.

[21] Ross PL, Huang YN, Marchese JN, Williamson B, Parker K, Hattan S, et al. Multiplexed protein quantitation in *Saccharomyces cerevisiae* using amine-reactive isobaric tagging reagents. Mol Cell Proteomics 2004;3:1154–69.
[22] Ong SE, Blagoev B, Kratchmarova I, Kristensen DB, Steen H, Pandey A, et al. Stable isotope labeling by amino acids in cell culture, SILAC, as a simple and accurate approach to expression proteomics. Mol Cell Proteomics 2002;1:376–86.
[23] Li Z, Adams RM, Chourey K, Hurst GB, Hettich RL, Pan C. Systematic comparison of label-free, metabolic labeling, and isobaric chemical labeling for quantitative proteomics on LTQ Orbitrap Velos. J Proteome Res 2012;11:1582–90.
[24] Merl J, Ueffing M, Hauck SM, von Toerne C. Direct comparison of MS-based label-free and SILAC quantitative proteome profiling strategies in primary retinal Muller cells. Proteomics 2012;12:1902–11.
[25] Hood JD, Cheresh DA. Role of integrins in cell invasion and migration. Nat Rev Cancer 2002;2:91–100.
[26] Filardo EJ, Brooks PC, Deming SL, Damsky C, Cheresh DA. Requirement of the NPXY motif in the integrin beta 3 subunit cytoplasmic tail for melanoma cell migration in vitro and in vivo. J Cell Biol 1995;130:441–50.
[27] Galliher AJ, Schiemann WP. Beta3 integrin and Src facilitate transforming growth factor-beta mediated induction of epithelial-mesenchymal transition in mammary epithelial cells. Breast Cancer Res 2006;8:R42.
[28] Lei Y, Huang K, Gao C, Lau QC, Pan H, Xie K, et al. Proteomics identification of ITGB3 as a key regulator in reactive oxygen species-induced migration and invasion of colorectal cancer cells. Mol Cell Proteomics 2011;10. M110.005397.
[29] Liapis H, Flath A, Kitazawa S. Integrin alpha V beta 3 expression by bone-residing breast cancer metastases. Diagn Mol Pathol 1996;5:127–35.
[30] Chen J, Zhang J, Zhao Y, Li J, Fu M. Integrin beta3 down-regulates invasive features of ovarian cancer cells in SKOV3 cell subclones. J Cancer Res Clin Oncol 2009;135:909–17.
[31] Partheen K, Levan K, Osterberg L, Claesson I, Fallenius G, Sundfeldt K, et al. Four potential biomarkers as prognostic factors in stage III serous ovarian adenocarcinomas. Int J Cancer 2008;123:2130–7.
[32] Partheen K, Levan K, Osterberg L, Claesson I, Sundfeldt K, Horvath G. External validation suggests Integrin beta 3 as prognostic biomarker in serous ovarian adenocarcinomas. BMC Cancer 2009;9:336.
[33] Wu Y, Zuo J, Ji G, Saiyin H, Liu X, Yin F, et al. Proapoptotic function of integrin beta(3) in human hepatocellular carcinoma cells. Clin Cancer Res 2009;15:60–9.
[34] Chu YQ, Ye ZY, Tao HQ, Wang YY, Zhao ZS. Relationship between cell adhesion molecules expression and the biological behavior of gastric carcinoma. World J Gastroenterol 2008;14:1990–6.
[35] Stupack DG, Puente XS, Boutsaboualoy S, Storgard CM, Cheresh DA. Apoptosis of adherent cells by recruitment of caspase-8 to unligated integrins. J Cell Biol 2001;155: 459–70.
[36] van der Flier A, Sonnenberg A. Function and interactions of integrins. Cell Tissue Res 2001;305:285–98.
[37] Chen YR, Juan HF, Huang HC, Huang HH, Lee YJ, Liao MY, et al. Quantitative proteomic and genomic profiling reveals metastasis-related protein expression patterns in gastric cancer cells. J Proteome Res 2006;5:2727–42.
[38] Schwanhausser B, Busse D, Li N, Dittmar G, Schuchhardt J, Wolf J, et al. Global quantification of mammalian gene expression control. Nature 2011;473:337–42.